# Effect of Moisture-Ingress on Adhesion Energy in a Metal Oxide-Polymer System

**Sheila Devasahayam**

*Steel Institute, University of Wollongong, Northfields Avenue, Wollongong N.S.W. 2522, Australia*

Received 8 July 2004; accepted 29 March 2005
DOI 10.1002/app.22588
Published online 6 December 2005 in Wiley InterScience (www.interscience.wiley.com).

**ABSTRACT:** This work quantifies the damage caused by moisture in a metal coating system under extreme weathering conditions, using Variable Radius Roll Adhesion Test (VaRRAT). Interfacial toughness (adhesion energy) between the metal oxide and the polymer in painted steel panels, studied by using VaRRAT, is observed to fall with increasing temperature and time of exposure to moisture. Possible cause for irreversible loss in adhesion energy in the paint system is attributed to the sorption of free water at the metal oxide–polymer interface. Different failure responses were observed in two different paint–metal systems. Adsorption or diffusion in the Henry's mode is rate controlling in green paints as indicated by the low activation energy of 12 kJ $mol^{-1}$. The white samples showed a high activation energy of 30 kJ $mol^{-1}$, indicating a mixed process of diffusion as well as chemical to be rate determining. Different paint/binder ratios are responsible for the different responses of these samples. © 2005 Wiley Periodicals, Inc. J Appl Polym Sci 99: 2052–2061, 2006

**Key words:** coatings; adhesion; glass transition; activation energy; pigments

## INTRODUCTION

A major requirement of a paint system on a metal substrate in a coating system is, besides serving the aesthetic purposes, to protect the metal against weathering and corrosion. The life of a paint–metal system is dependent, among other things, on its water uptake and resistance to hydrolysis. The dissolved oxygen and ions such as chlorides and sulfates in water contribute to osmotic swelling of the paints as well as the corrosion of the metal, causing reduction in adhesion energy and delamination, thus posing a serious threat to the life of these painted metal systems.[1]

Water uptake in paint systems depends on factors such as the solubility and solubility coefficient of water in the paint and the chemical structure and the morphology of the polymers and other additives used in the paint system. High concentrations of polar functional groups promote increased sorption of polar penetrants, water included.[2,3] The available functional groups in the polymer are determined by the extent of cure.

Moisture and high temperatures cause changes in the internal stresses in the coating systems.[4] Swelling by water causes tensile internal stresses,[5,6] and the variation in temperature causes thermal internal stresses.[7,8] These internal stresses cause coating defects under practical weathering conditions, and consequently, affect both the wet adhesion and the recovery of adhesion after the evaporation of water.

Water vapor transmission through a coating system involves different processes such as desorption/adsorption on the surface, dissolution in the polymer matrix, and diffusion through the polymer and oxide layers. Each of these processes are characterized by different activation energies.

Nguyen and Martin[9] ascribed the water-induced adhesion loss in an epoxy-steel system to the presence of multiple layers of water at the coating to steel interface. The presence of a water layer at the organic coating/iron oxide interface is due to the weak secondary bonds between the organic film and the iron oxide. The hydrogen bonding that occurs between a typical paint film and a steel surface has little resistance against water, particularly in an alkaline environment.[9,10] The bond energies of these weak secondary organic films to oxide bonds are less than 25 kJ $mol^{-1}$and the affinity of water to the high-energy polar iron oxide surface is around 40–60 kJ $mol^{-1}$.[11,12] Kinloch[13] also observed, based on thermodynamic analysis, that the polymer-to-metal oxide interfacial bonds are not stable in an aqueous medium and that the water is capable of displacing the organic film from the substrate.

Typical polymer coatings for metals are based on polyester, epoxy, acrylic, or fluoropolymer systems. Each of these paint systems has different water absorbing, dirt shedding, and radiation-resistance properties.

*Correspondence to:* S. Devasahayam (s47_d@hotmail.com).

**TABLE I**
**Description of the Samples Used**

| Samples | Substrate thickness (mm) | Primer thickness ($\mu$m) | Topcoat thickness ($\mu$m) | Resin type |
|---|---|---|---|---|
| Green | 0.47 | 5 | 18 | Epoxy; polyester |
| White | 0.47 | 5 | 18 | Epoxy; polyester |

The paint system used in the present study is epoxy and polyester based. In an epoxy system, the presence of high concentrations of tertiary amine increases the water solubility as opposed to low concentrations of tertiary amines.[14] A high concentration of hydrophilic hydroxyl groups along the backbone also increases the water uptake. However, with an increasing mono-epoxy/di-epoxy ratio, or in an undercured epoxy system, a decrease in solubility coefficients, and an increase in diffusion coefficients and molar energies for water, is reported.[15]

Polyester systems contain less polar ester moieties and consequently are less hydrophilic than epoxy systems. Structure of the polyester is reported to play a key role in determining the moisture uptake in these systems.[16] For example, vinyl esters are more stable to hydrolysis than isopolyesters, due to the fact that the ester linkages in the vinyl esters are terminal and are shielded by the methyl groups. When the ester groups in polyesters are distributed along the main chain, they are more vulnerable to hydrolysis.[16] Resistance to hydrolysis is expected to increase with increase in number of $CH_2$ groups in the acid component.

The present study explores the changes that occur in paint–metal oxide coating systems due to prolonged exposure to water under extreme weathering conditions using Variable Radius Roll Adhesion Test (VaRRAT).[17] The main objective is to understand long-term adhesion and adhesion-related properties in the painted steel based on VaRRAT results.

## EXPERIMENTAL

### Samples

The sample characteristics are given in Table I. The entire coating system is illustrated in Figure 1. The sample system consists of a substrate of 0.47-mm-thick steel sheet, coated with 20-$\mu$m, zinc-aluminum alloy; 5-$\mu$m, epoxy-based primer; and 18-$\mu$m melamine-crosslinked polyester topcoat. Two different topcoats representative of a low-resin/pigment ratio system (colored white) and a high-resin/pigment system (colored green) are chosen for the present study. The lighter colors generally have a higher pigment loading than the darker colors. The pigments present in the samples are mostly mixed metal oxide ceramics. The white samples comprise mainly of $TiO_2$-based pigments. The interactions of these pigments with the polymer network is assumed to depend only on the resin/pigment ratio in the present study. Estimation of the exact crosslink density of these paints is not straightforward because of the presence of these pigments, fillers, and the flatting agents in the sample. The storage modulus of the paint was estimated[18] to be $\sim 18$ MPa, and the crosslink density is roughly estimated[19] by using the above storage modulus as $\sim 2.0 \times 10^6$ mol/m$^3$. This value does not account for the fillers and the pigments present in the paint layer.

### Control samples

The control samples are dry samples exposed to the experimental temperatures in an oven, but not to moisture.

### Weathering tests

The painted panels as received were exposed to a constant condensing humidity of 95% at different temperatures (300, 313, 328, and 341 K) in a fluorescent, ultraviolet and condenser unit (QUV)-accelerated weather tester (in a condensation mode only, i.e., no

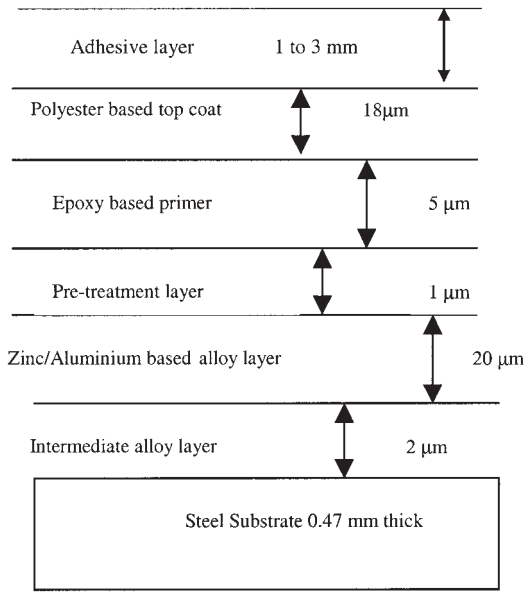


**Figure 1** The coating system.

UV light cycle) and a Cleveland condensation tester, for a required time at the experimental temperatures.

The QUV Accelerated Weather Tester exposes the samples to alternating cycles of light and moisture, at controlled, elevated temperatures. In a few days or weeks, the QUV Accelerated Weather Tester can reproduce damage that occurs over months or years of being outdoors. (The UV-A 340 lamps, not used in the present study, provide the best available simulation of sunlight in the critical, short wavelength region from 315 to 400 nm.) Exposure of tests samples from between 500 and 2000 h provides a good representation of an environment's most detrimental effects on a material.

The Cleveland humidity test, developed by the Cleveland Society for Coatings Technology, establishes high humidity from a heated water supply in the base of the test cabinet. This test is carried out in accordance with The American Standard, ASTM D 4585-92 Standard Practice for Testing Water Resistance of Coatings Using Controlled Condensation," and is similar to ISO 6270, in that the test coatings form the cover for the test cabinet. The operating temperature, however, can be adjusted in the range 38–82°C. There must be a temperature differential between the cabinet air temperature and the room temperature of at least 11°C, to ensure that condensation takes place on the test faces.

In the present study, the QUV weather tester was operated in the condensation mode at 55 and 68°C, and Cleveland tester was operated at 27 and 40°C. Moisture was prevented from getting through the edges of the samples by sealing with Silastic 732 (a silicone sealant).

### Variable radius roll adhesion test (VaRRAT)[17]

The adhesion energy of the samples exposed to moisture over a period of time at different temperatures was calculated from the measured critical radius at room temperature by using the VaRRAT.[17] This test relies on the application of a reinforcing layer of epoxy resin over the painted side of a narrow strip of the coated metal. The sample is locked into the roll at the low radius of curvature section and the steel substrate is rolled away from the epoxy resin propagating a crack somewhere within the paint system, or at the metal–primer interface. The loading configuration drives the crack preferentially toward the steel rather than into the epoxy resin. The epoxy resin overlay provided sufficient stiffness to cause the crack to propagate when the steel is rolled around an appropriate radius. The parameters measured were the critical roll radius (critical radius occurs when the crack propagates around steadily increasing radii until it finds some critical radius at which insufficient energy is stored in the epoxy resin to drive it further. Smaller critical radii represent stronger adhesion energies), which is a function of the epoxy resin thickness.

#### Epoxy resin cure

The diglycidyl ether of bisphenol A based epoxy resin used in the present study was Ciba-Geigy (two-part epoxy) K106. The resin (AW106) to hardener (HV 953U) ratio was 100 to 80 w/w. The paint panels were then cut to 300 × 24 mm strips for the adhesion tests. The samples were wiped clean with alcohol, and Ciba-Geigy K106 epoxy resin was poured over a casting tray containing the samples and two dog-bone molds. The samples were placed in an oven at 50°C for 24 h. A 50°C cure temperature was used so as to minimize the thermal mismatch stress when the samples cooled due to the differing thermal expansion coefficients of the steel and the epoxy resin. A low-temperature cure cycle is not expected to cause additional paint cure or change in the paint properties. After curing, the samples were machined to the required dimensions. The adhesive layer thickness varied between 1 and 3 mm. The dog-bone samples, with the dimensions of 100 × 13.58 mm ± 0.14 × 2.46 ± 0.04 mm were used to determine Young's modulus of the bulk epoxy resin overlay. Residual stresses of the epoxy overlay measured from the radius of the curvature of the sample was in the order of 5 $Jm^{-2}$. The measurement of mechanical properties of the epoxy overlay was carried out by using an Instron 4302 testing machine. The Young's modulus was calculated from the stress–strain curves under uniaxial tension up to a strain of 0.1 at strain rate of 3%/min.[17]

The adhesion energy is calculated as $G = G_b + G_p$, where $G_b$ is the bending adhesion energy and $G_p$ is the Poisson's adhesion energy given as

$$G_b = \frac{E^2}{2E_u}\int_0^H \left(\frac{(h_s + 2x/h_s + 2R)}{1 + D(h_s + 2x/h_s + 2R)}\right)^2 dx$$

$$G_p = \frac{E^2}{2E_n}\int_0^H \left(\frac{\nu(h_s + 2x/h_s + 2R)}{1 + D\nu(h_s + 2x/h_s + 2R)}\right)^2 dx$$

where $R$ is critical radius (m); $D$ is the shape factor; $E$ is the loading modulus (MPa); $H$ is epoxy layer thickness (m); $E_u$ is the unloading modulus (MPa); $h_s$ is the thickness of the substrate (m); and (Poisson's ratio) is 0.37. The values of $E$ and $E_u$ were experimentally determined in this study from the stress–strain relationship of the bulk epoxy. $D$, the shape factor, is the fitted parameter obtained by using the classic equation

$$\sigma = E\frac{\varepsilon}{1 + D\varepsilon}$$

where $\sigma$ is stress (Pa) and $\varepsilon$ is engineering strain.[17]

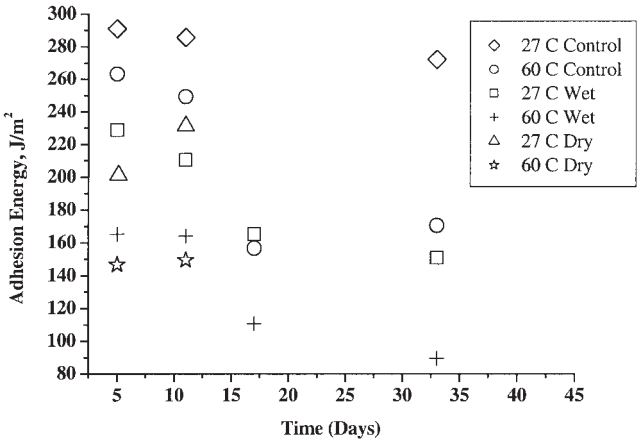


**Figure 2** Effect of moisture on adhesion energy with respect to time and temperature (green samples).

### Glass transition temperature ($T_g$) measurements

Changes in $T_g$ (onset temperature of bulk softening) due to the moisture uptake were determined by the probe-penetration depth by using thermal mechanical analysis (TMA). The measurements were carried out on a Perkin–Elmer TMA-7, operating with a 1-mm-diameter hemispherical probe, at a heating rate of 10°C/min, and probe force of 50 mN under $N_2$.

### ATR-FTIR measurements

The chemical changes occurring in the paint system due to the exposure to moisture were determined by using ATR-FTIR (Nexus 870, DTGS TEC). Sixty-four scans were taken with 64 background scans at a resolution of 4 $cm^{-1}$.

## RESULTS

### Adhesion energy

VaRRAT results [Figs. 2 and 3(A)] showed higher adhesion energy, $G$, for the green samples compared to the white samples. The failure for the green was observed at the metal–primer interface (adhesive failure). White samples exhibited cohesive failure within the topcoat. The difference is attributable to the greater amount of pigments present in the white topcoat compared to the green. The adhesive–paint interface never failed. Adhesion energy, $G$, as determined by VaRRAT, was found to vary with respect to time and temperature of exposure for both the green as well as the white samples. Average results of a set of three adhesion experiments, for each sample, are presented in Figure 2 for green samples and in Figure 3(A) (wet and control samples) and Figure 3(B) (dry and control samples) for white samples. The initial adhesion energies (time = 0) for green samples were 295 $Jm^{-2}$ and for the white samples, 170 $Jm^{-2}$.

Figures 2 (green samples) and 3(A, B) (white samples) indicate that the adhesion energies for both the white and the green samples decreased with increasing time and temperatures. However, the adhesion failure in the green samples was more rapid under similar experimental conditions compared to in the white samples [e.g., for 60°C green samples the loss in adhesion energy after ~ 30 days is ~ 200 $Jm^{-2}$ (approximately 68%), while for 68°C white samples it is ~ 45 $Jm^{-2}$ ~ 26%].

### Dry samples

Both white and green samples allowed to dry at ambient conditions after their exposure to humidity did not recover their original adhesion energy.

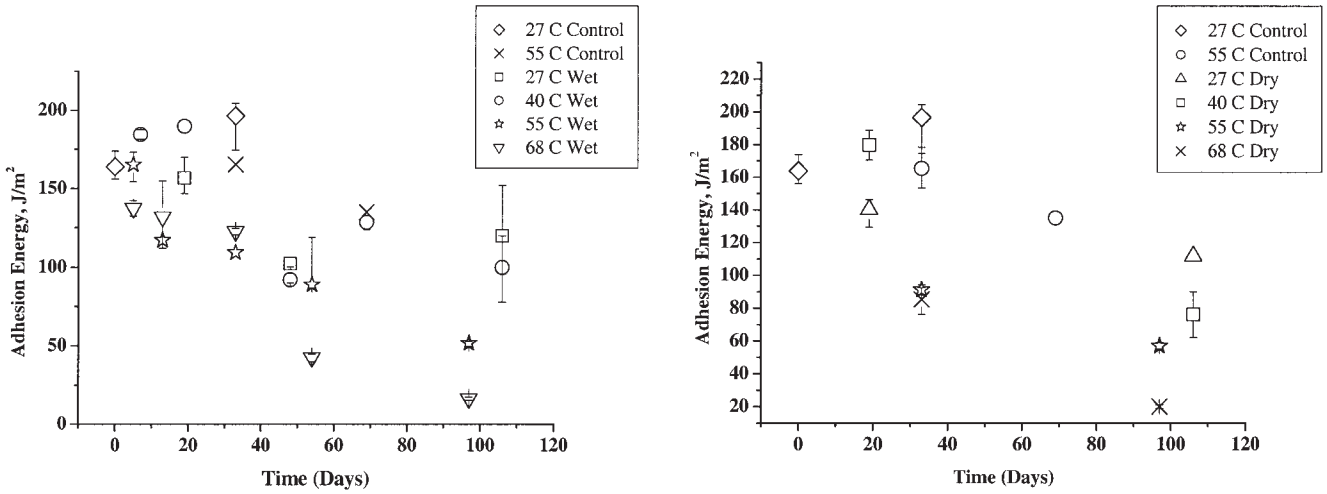


**Figure 3** (A) Effect of moisture on adhesion energy with respect to time and temperature (white samples, wet). (B) Effect of moisture on adhesion energy with respect to time and temperature (white samples, dry).

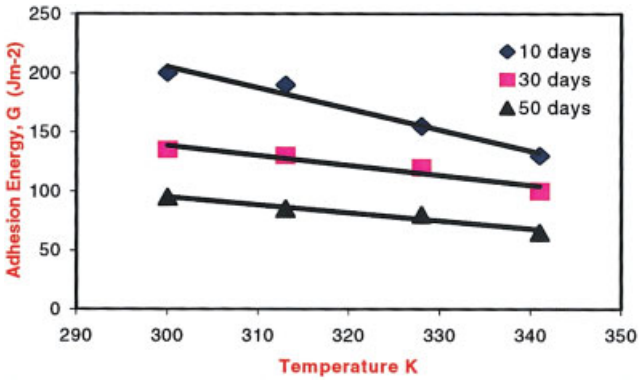


**Figure 4** Temperature dependence of adhesion energy of white samples for various immersion times. [Color figure can be viewed in the online issue, which is available at www.interscience.wiley.com.]

## Control samples

The control samples also experienced loss in adhesion energy [Figs. 2 and 3(A, B)]. The loss in adhesion energy was higher for the samples exposed to higher temperatures. When the $T_g$ of the sample is below the experimental temperature, the adhesion bonds can slide at the substrate surface, even in the absence of water, facilitating the stress relaxation by bond sliding, and adversely affecting the adhesion energy. However, if the $T_g$ is sufficiently above the experimental temperature, the adhesion bonds are immobile and fixed to the substrate, with no effect on the adhesion energy. The variation in temperature can cause thermal internal stresses[7,8] as already mentioned. These internal stresses cause coating defects, thus affecting the adhesion energy.

Though the loss of solvent in the sample was not measured, it is also possible that the loss in low molecular weight volatile products and/or the residual solvents can contribute to loss in the adhesion energy, especially above the $T_g$ of the paint samples, when transition from glassy state to liquid state of the polymer/paint favors evaporation of the volatile products. Because the volume contraction accompanying the solvent evaporation is not uniform throughout the polymer matrix, for example, the paint layer near the surface of the substrate may not experience the same rate of contraction as that of the paint at the top layer, this leads to compressive internal stress, and consequently, loss in adhesion.

## Kinetics and mechanisms

A negative linear temperature dependence of the adhesion energy for the white samples is indicated in Figure 4, with the slopes of the curves decreasing with the increasing time of exposure.

To determine the rate constants, $K$, for adhesion loss as a function of time, the functions of fraction transformed, $f(\alpha)$, are plotted against the time as shown in Figure 5(A, B). The fraction transformed is defined by the relation: $(\alpha) = [G(0) - G(t)]/G(0)$, where $G(t)$ represents the adhesion energy at a given time and $G(0)$ represents the adhesion energy when $t = 0$. [$G(0)$ is the initial adhesion energy of the sample as received, and not that of the control samples.] The term $G(0) - G(t)$ represents the overall loss in adhesion energy at time $t$, which includes the adhesion loss due to high temperature effects as well as the humidity effects. $K$ is defined as the slope of $f(\alpha)$ versus time curve. Because the $(\alpha)$ versus time relationship was

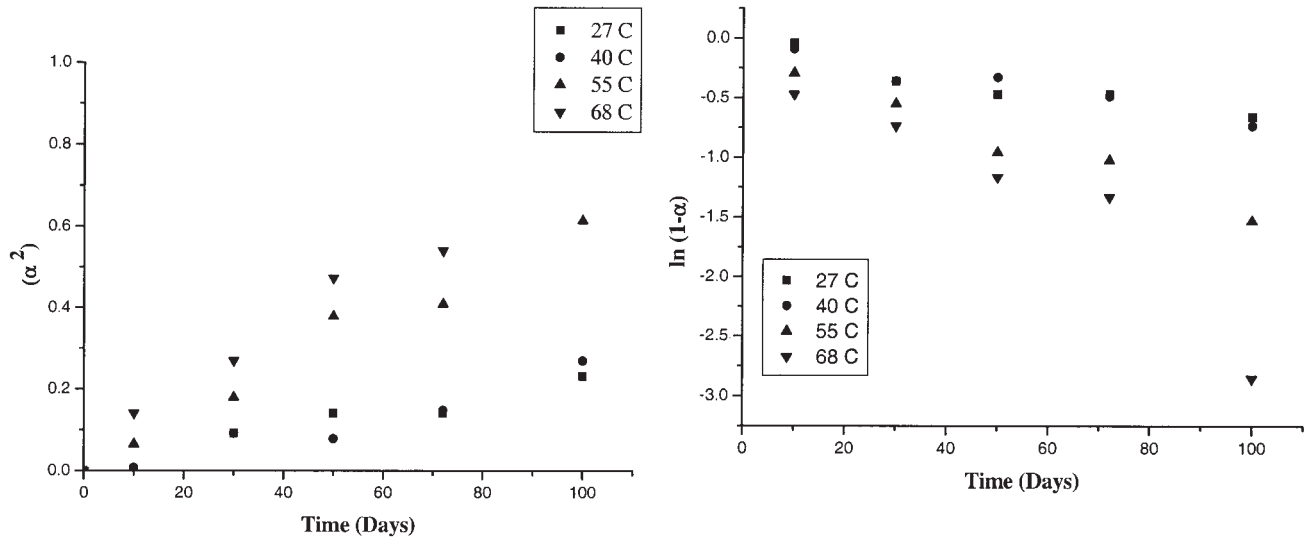


**Figure 5** A. Plot of $(\alpha^2)$ versus time (white samples). (B) Plot of $\ln(1 - \alpha)$ versus time (white samples).

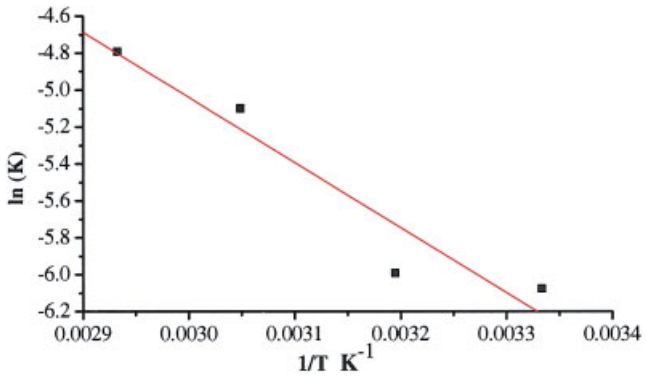


**Figure 6** Activation energy for adhesion loss in white sample, plot of ln(K) versus $1/T$. [Color figure can be viewed in the online issue, which is available at www.interscience.wiley.com.]

not linear, different reaction models were used to linearize the curves. The surface reaction models, $1 - (1 - \alpha)^{1/Fp}$, which reduces to ($\alpha$) versus time, for the shape factor, $Fp = 1$, for a planar substrate; and ln($1 - \alpha$) versus time, did not yield linear plots. The diffusion and mass transfer model, ($\alpha^2$) versus time, however, yielded linear plots for both the green and the white samples.[20]

The $K$ values calculated by using the diffusion models for green samples for similar experimental temperatures were higher than those for the white samples.

Figure 6 shows the linear plot of ln($K$) versus the inverse temperature for the white samples, for diffusion models the slopes of which yielded an activation energy equal to 30 kJ mol$^{-1}$. The fitted parameters for the linear model were the slope, $-3500 \pm 750$ the intercept, $5.60 \pm 2.0$, and the $R^2$, 0.92. The activation energy obtained by using the diffusion model for the green samples was 12 kJ mol$^{-1}$.

### TMA measurements

Figure 7 shows the TMA curves for the white samples as received and the samples exposed to the humidity at different temperatures. The TMA curves show transition corresponding to the $T_g$ (28°C) of the topcoat, but not the transition corresponding to the $T_g$ (80°C) of the primer underneath the topcoat, probably due to the higher proportion of the topcoat to the primer ($18:5$ $\mu$m). The sample exposed to 68°C showed a slight decrease in $T_g$.

Although $T_g$ is expected to decrease because of the exposure to moisture, the present study did not show much variation in the $T_g$ (except for the slight decrease shown by the sample exposed to the humidity at 68°C). The swelling in the polymer matrix caused by the absorption of water (decreasing $T_g$) perhaps compensates the shrinkage of the polymer matrix caused by solvent evaporation (increasing $T_g$) to a degree. The dimensional change caused by the plasticization by moisture such as network disruption and the swelling of the matrix is limited by the presence and the orientation of the fillers, flatting agents, and the pigments in the paints and the flow direction of the moisture. At higher temperatures, the water molecules can enter the film more rapidly and take up position between the chains of polymer. Increasing the temperature also increases the diffusion coefficient of water for a given polymer matrix. There, the water will act as plasticizers for the film, actually depressing the $T_g$. This drop will facilitate further absorption of water into the paint matrix.

The probe penetration depth seemed to increase as the time of exposure increased, especially for 68°C, indicating network disruption or swelling of the polymer matrix. However, it should be noted that, although the probe penetration depth gives a good indication of the network integrity in the polymer matrix, presence of flatting agent in the polymer matrix is expected to hamper the probe penetration.

### FTIR

Figure 8(A, B) shows the ATR-FTIR spectra of white samples exposed to the 95% relative humidity at 55°C for 97 days, samples allowed to dry naturally (dry) after exposure to moisture and the control sample not exposed to moisture but just kept in the oven at 27°C. The only chemical change perceived is in the $CH_2$ region, 2965 and 2928 cm$^{-1}$. The intensity for the asymmetric stretch for $CH_3$ (2965 cm$^{-1}$) has increased, whereas asymmetric stretch for $CH_2$ has decreased. It is possible that, due to the free volume change caused

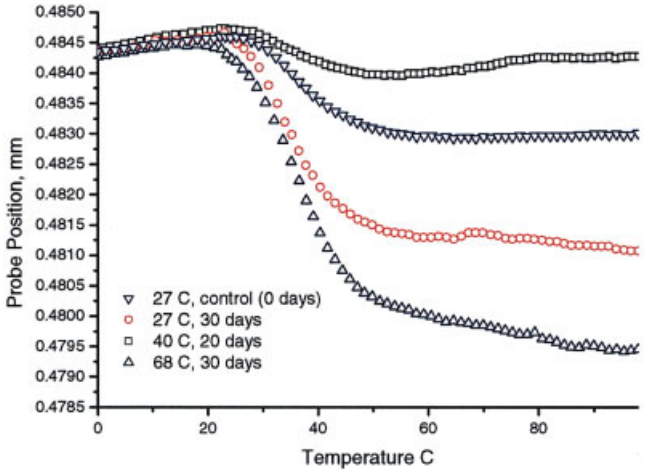


**Figure 7** TMA curves for the white sample exposed to moisture at different temperatures. [Color figure can be viewed in the online issue, which is available at www.interscience.wiley.com.]

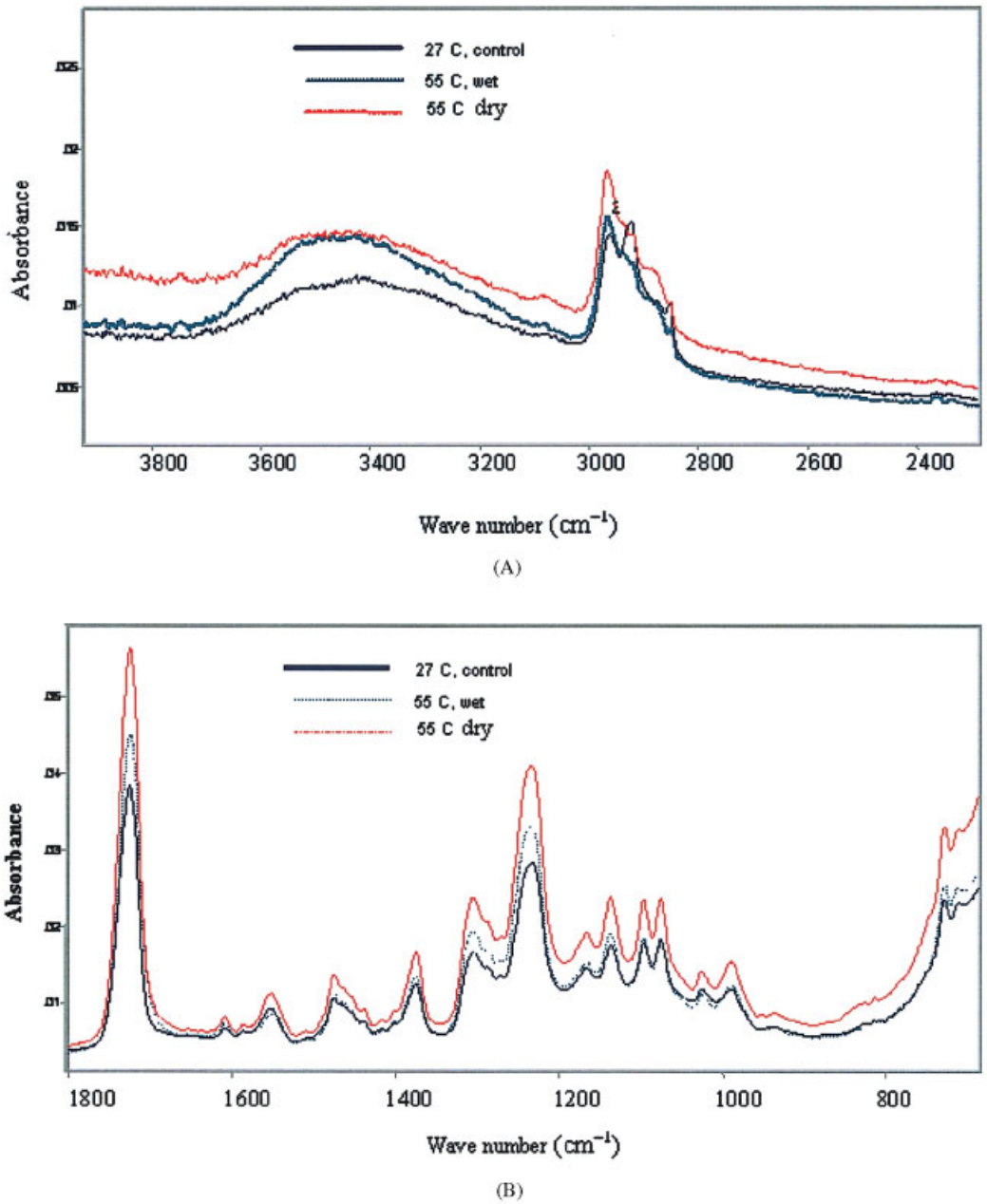


**Figure 8** (A) ATR spectra of white samples (control, 55°C; wet, 55°C dry). (B) ATR spectra of white samples (control, 55°C; wet, 55°C dry). [Color figure can be viewed in the online issue, which is available at www.interscience.wiley.com.]

by the plasticizer ($H_2O$) in the system, the $CH_2$ experiences restricted mobility/stretches, while the terminal $CH_3$ might have more freedom than $CH_2$.

## DISCUSSION

The experimental conditions were such that all the top-coated samples were exposed to humidity at temperatures equal to or above the initial glass transition temperatures of the polyester, the topcoat (~ 28°C), but below the initial glass transition temperature of the epoxy, the primer (~ 80°C). This would imply that the samples could be at two different states [i.e., glassy (due to epoxy primer) and mobile (due to polyester topcoat)] at lower experimental temperatures.

Diffusion of water through the paint system is governed by physical characteristics of a polymer such as crosslink density, cohesive energy density, and the rigidity of the chains.[15] At 60°C the reported diffusion coefficients of water in polyester and epoxy are in the following order: isopolyester > vinyl ester > epoxy.[21] The water diffusion through the primer is expected to

be rather slow compared to through the topcoat. In fact, because the experimental temperature is lower than $T_g$ of the primer, the water in the primer layer would be in a less-mobile state. It is reported, however, that water and oxygen are capable of fitting easily into free volume cavities in epoxy facilitating plasticization by water, as the dry mean void diameters of the crosslinked epoxy coatings range from ~ 5 to 6 Å, and the kinetic diameters of $H_2O$ and $O_2$ are only 2.65 and 3.46 Å, respectively.[22]

It is possible that the thickness of the topcoat, being about 3.5 times greater than the primer thickness of 5 $\mu$m, could hamper water transport across the topcoat compared to across the primer layer. The swelling of the polymer network caused by the absorption of water can cause depression in the $T_g$ of the topcoat, allowing the water to diffuse up to the primer layer. The epoxy primer layer is more hydrophilic than the polyester system (topcoat), which comprised less polar ester moieties, and the absorbed moisture can depress the $T_g$ of the epoxy primer layer further, allowing the water to permeate through to the metal surface. However, this effect will be more pronounced in the green samples with a low pigment/resin ratio rather than in the white sample with a high pigment/resin ratio. This is demonstrated by the planes of fracture, which is the metal–primer interface (adhesive) for the green samples and within the top coat for the white samples. The excess pigments in the white samples provide better barrier properties.

### Free water and bound water

Dual modes of sorption of water, namely, Henry's law sorption (bound water), and Langmuir sorption (free water; water immobilized in microvoids), occur in a polymer.[23,24] Local equilibrium between the two modes is maintained throughout the matrix. Though diffusion occurs mainly in the Henry's mode, the Langmuir population is also reported have partial mobility. The terms free water and bound water do not apply to bulk water. The bound water is a reversible thermodynamic quantity and its temperature dependence is described by a negative value of the exothermic heat of sorption in Henry's law. The amount of bound water decreases with increasing temperature. The free water and the bound water can be quantified by using nuclear magnetic resonance (NMR) relaxometry or quasi-elastic neutron scattering measurements. Due to practical difficulties, these experiments were not carried out. However, it was hoped that the $T_g$ measurements, the adhesion measurements, and the activation energy for the loss of adhesion energy would shed some light on the roles of free water and bound water in the present system.

Depression in $T_g$ is related to the hygrothermal history.[25] The amount of the bound water in a system is reported to be proportional to the depression in $T_g$.[26,27] The sorbed moisture depresses the $T_g$ by plasticizing the polymer network, thus affecting the mechanical performance and durability.[23] The present study showed little change in $T_g$, indicating the role of bound water in these systems to be negligible. However, the disruption of network observed in the TMA plots (Fig. 7) indicated plasticization of the polymer network.

The free water sorption is reported to increase with increasing temperature in an irreversible way. The ratio of the bound water to free water is reported to be 9 : 1 at 300 K.[28] Even at the highest temperature (95°C) the amount of bound water exceeds the amount of free water.[23] Free water is assumed to be immobilized by irreversible microcavitational damage. The activation energies for sorption of the bound water and the free water are reported to be $-1.37$ and 12.28 kJ mol$^{-1}$, respectively.[23]

In a water–solid (alumina) system, bond energies corresponding to adsorption and capillary condensation have the values of the order of 10–25 kJ mol$^{-1}$, and for chemical bonding, the values are ~ 45–60 kJ mol$^{-1}$.[29] For a ZnO–water system, the chemical interaction energy is reported to be 46 kJ mol$^{-1}$.[30] For a relatively immobile monolayer of water in a ZnO system, however, the activation energy is reportedly 10.7 kJ mol$^{-1}$. The immobile monolayer of water is caused by a decrease in the activation energy because of the limitation on paths for molecular motion of monolayer water by impermeable crystal surface. Formation of hydrogen bonds in this state is hindered by strong perturbation from the incommensurate surface field, resulting in low activation energy of ~ 10 kJ mol$^{-1}$.[29]

The activation energy, 12 kJ mol$^{-1}$, found in the present study for green samples points towards the activation energy for the sorption or diffusion for Henry's process.[23] The activation energy, 30 kJ mol$^{-1}$, for white samples is higher for a physical process obeying Henry's law, although activation energy reported for processes such as diffusion[31] and permeation of water[32] in and through the polymer are ~ 36 kJ mol$^{-1}$ (for a polyester system) and 15–58 kJ mol$^{-1}$ (composition-dependent activation energy), respectively. For sulfur, diffusing through epoxy, a diffusion coefficient as high as 71 kJ mol$^{-1}$is reported.[33] This high observed value reflects both physical process as well as chemical reaction. The large size of the sulfur atom is also cited as one of the reasons.[33] Similarly, a high activation energy for white samples could perhaps indicate both diffusion and chemical process as rate determining.

The irreversible loss observed in adhesion energy in the present study is attributed to the changes caused by the free water in the microvoids. Despite $T_g$ values remaining close to that of the original samples, the net work disruption points towards the free water as the

cause for the adhesion failure. However, is it the free water sorption involving the polymer–water interface or metal–water interface or both? The white samples exhibited cohesive failure (i.e., failure within the paint layer). This may be due to the excess pigments present in the white samples. The free water at the metal oxide–water interface (as most of the pigments are metal oxides) perhaps causes cohesive failure.

The lower activation energy for adhesion failure in green samples compared to white samples may be associated with higher tensile internal stresses caused by the swelling of the polymer matrix due to adsorption in Henry's mode, compared to the white samples, where high amount of pigments in the polymer matrix would inhibit the swelling/tensile internal stresses caused by water. The activation energy for white samples and the green samples correspond to 0.50 $Jm^{-2}$ (30 kJ $mol^{-1}$) and 0.20 $Jm^{-2}$ (12 kJ $mol^{-1}$) based on the approximate number polymer chains crossing at the interface[34] $\sim 10^{18}$. The high activation energy observed for the white samples implies that they have better mechanical properties compared to the green samples, because of the presence of excess pigments, which increase the effective modulus. The pigments also act as crack stoppers, inhibiting crack propagation, requiring higher load to extend the polymer chain to its critical length across the interface to effect the debonding or delamination. The low activation energy in the green samples implies that the debond mechanism aided by the plasticization or swelling by water could be a physical process such as chain pullout, whereas a higher activation energy in the white samples, where the degree of plasticization is less compared to the green samples because of the presence of the pigments, the debond mechanism could involve the chain scission mechanism as well.

## CONCLUSIONS

Adhesion failure is observed at the metallic coating to primer interface for the green samples, indicating that water has permeated through to the metal surface. Green samples showed a higher rate of adhesion failure upon exposure to moisture compared to the white samples. The green samples showed adhesive failure, whereas the white samples exhibited cohesive failure. This is attributed to the excess pigments present in the white samples. Presence of the free water at the metal oxide–water interface is the cause for cohesive failure in the white samples.

The activation energy for the adhesion failure of $\sim 12$ and 30 kJ $mol^{-1}$, respectively, for green and white samples points towards processes involving Henry's diffusion process (for green), and combined diffusion, free water, and chemical process (for white) to be the rate-determining steps.[9,10] The permanent loss in adhesion energy points towards free water sorption at the paint–metal interface. The low activation energy for the green samples is probably due to chain pullout mechanism aided by the plasticization or swelling of the polymer matrix to cause delamination. The high activation energy in white samples could involve chain scission mechanism as well as the free water at the pigment–polymer interface to cause the delamination.

The author thanks the following people: Prof. Hugh Brown, University of Wollongong, Australia, for the overall discussions; Dr. David Buxton, Bluescope Steel, Australia for experimental facilities; Dr. Peter Fredericks, QUT, Australia, for measurements and discussions on ATR-FTIR; Pat Smith, Bluescope Steel, Australia for assistance with Cleveland and QUV, TMA measurements, and sample preparation; and Dr. Chris Fellows, University of Sydney, Australia for comments. Support of the ARC-linkage scheme is acknowledged.

## References

1. Roobol, N. R. Roobol on Painting Salts Cause Corrosion; Industrial Paint and Powder Web site search archives; www.ippmagazine.com/search.htm
2. Nicodemo, L.; Bellucci, F.; Marcone, A.; Monetta, T. J Membr Sci 1990, 52, 393.
3. Danieley, N. D.; Long, R. E. J Polym Sci: Polym Chem Ed 1981, 19, 2443.
4. Negele, O.; Funke, W. Prog Org Coat 1996, 28, 285.
5. Nilsson, E. Farg Och Lack 1975, 21, 318.
6. Perera, D. Y.; Vanden Eynde, D. 16th FATIPEC Congress Book 1982, 129.
7. Sato, K. Prog Org Coat 1980, 8, 143.
8. Shimbo, M.; Ochi, M.; Arai, K. J Coat Technol 1984, 56, 713.
9. Nguyen, T.; Martin, J. W. In Modes and Mechanisms of Degradation of Epoxy-Coated Reinforcing Steel in a Marine Environment, Durability of Building Materials and Components; Sjostrom, C., Ed.; E&FN Spon: UK, 1996; Vol. 1, p 7.
10. Murase, M.; Watts, J. F. J Mater Chem 1988, 8, 1007.
11. Bollger, J. C.; Michaels, A. S. Molecular structure and electrostatic interactions at polymer–solid interface; In Interface Conversion for Polymeric Coatings; Elsevier: New York, 1969; pp 3–60.
12. Thiel, P. A.; Madey, T. E. Surf Sci Rep 1987, 7, 211.
13. Kinloch, A. J In Durability of Structural Adhesives; Applied Science Publishers: New York, 1983; pp 1–38.
14. Carfagna, C.; Apicella, A.; Nicolais, L. J. Appl Polym Sci 1982, 27, 105.
15. Damian, C.; Escoubes, M.; Espuche, E. J Appl Polym Sci 2001, 80, 2058.
16. Chin, J. W.; Nguyen, T.; Aouadi, K. J Compos Tech Res 1997, 19, 205.
17. Jinks, D.; Brown, H.; Buxton, D. J Coat Technol 2002, 74, 49.
18. Devasahayam, S. J Polym Sci, Part B: Polym Phys 2004, 42, 3822.
19. Hill, L. W. Prog Org Chem 1997, 31, 235.
20. Sohn, H. Y.; Wadsworth, M. E., Eds. Rate Processes Phenomena of Extractive Metallurgy; Plenum Press: New York, 1979.
21. Chin, J. W.; Nguyen, T.; Apuadi, K. J Appl Polym Sci 1999, 71, 483.
22. MacQueen, R. C.; Granata, R. C. Prog Org Coat 1996, 28, 97.

23. Suh, D. W.; Ku, M. K.; Nam, J D. J Compos Mater 2001, 35, 264.
24. Vieth, W. R. Diffusion in and through Polymers: Principles and Applications; Oxford University Press: New York, 1991.
25. Choi, H. S.; Ahn, K. J.; Nam, J-D.; Chun, H. J Composites, Part A 2001, 32, 709.
26. Zhang, Z.; Britt, I. J.; Tung, M. A. J Polym Sci: Polym Phys Ed 1999, 37, 691.
27. Karasz, P. In Water in Polymers; Rowland, S. P., Ed.; American Chemical Society: Washington, DC, 1980.
28. Balasubramanian, S.; Pal, S.; Bagchi, B. Condensed Matter, abstract cond-mat/0302069 http://arxiv.org/abs/cond-mat/0302069.
29. Sinitsky, A. S.; Ketsko, V. A.; Pentin, I. V.; Murav'eva, G. P.; Il'inskii, A. L.; Oleynikov, N. N. Russ J Inorg Chem 2003, 48, 406.
30. Takahara, S.; Kittaka, S.; Mori, T.; Kuroda, Y.; Yamaguchi, T.; Shibata, T. J Phys Chem B 2002, 106, 5689.
31. Marais, S.; Metayer, M.; Nguyen, T. Q.; Labbe, M.; Saiter, J. M. Eur Polym Mater 2000, 36, 453.
32. Kumar, R. S.; Auch, M.; Ou, E.; Ewald, G.; Jin, C. S. Thin Solid Films 2002, 417, 120.
33. Berry, B. S.; Susko, J. R. Polymers 1977, 21, 176.
34. Ghatak, A.; Vorvolakos, K.; Hongquan, S.; Malokty, D. L.; Chaudhury, M. K. J Phys Chem B 2000, 104, 4018.